ISTITUTO NAZIONALE DI FISICA NUCLEARE

Sezione di Milano

INFN/AE-95/03
20 Gennaio 1995

G. Bellini:

CHARM SPECTROSCOPY AND LIFETIME

PACS: 14.65.Dw

SIS-Pubblicazioni
dei Laboratori Nazionali di Frascati

INFN - Istituto Nazionale di Fisica Nucleare
Sezione di Milano

INFN/AE–95/03
20 Gennaio 1995

CHARM SPECTROSCOPY AND LIFETIME

G. Bellini:

Dipartimento di Fisica dell'Università e INFN–Sezione di Milano,
Via Celoria 16, I–20133 Milano, Italy

Abstract

A review of the charm state lifetimes and of the charm baryon masses is presented. The $\frac{\tau(D^{\pm})}{\tau(D^0)}$ and $\frac{\tau(D_s^{\pm})}{\tau(D^0)}$ are now known with an accuracy of 1.7% and 3.6%, respectively, and the baryon lifetime hierarchy seems well established. The measurements of the Ω_c^0 mass converge to a value in the range $2700 - 2710\ MeV/c^2$.

1 Introduction

In the last two years a large improvement has been achieved in the charm particle lifetime. The E687 data gave a very important contribution.
In this paper I am trying to give an up to date picture of the status of the art in this field.
The paper consists of four sections. In the first I discuss the methods adopted to measure the times of life and to fit the mean lifetime value of the charm states. In the sections 2. and 3. I discuss the lifetime measurements of the charmed mesons and baryons and the mass values of the charged and neutral cascades and Ω_c^0. Finally in the fourth section I will present some conclusions.

2 Lifetime measurement

The distance $\ell = \beta\gamma ct = \frac{P}{M}ct$ has to be measured for each charm state. Due to the short τ_c $[10^{-12} - 10^{-13}s]$, the measurements depend crucially upon the spatial resolution. Then a high precision vertex detector is needed. Just as an example the resolution of the E687 microvertex detector is $\sigma_l \simeq$ few hundreds of microns and $\sigma_t \simeq$ few tens of microns.

2.1 Vertexing

As it is well known two different approaches can be used to reconstruct the vertices: the "stand alone" and the "candidate driven" approach.
The "stand alone" method starts with an hypothesis for the primary vertex, then removes worst tracks and looks for a secondary vertex with the rejected tracks.
In the "candidate-driven" method, first the charm candidate forms a "seed" track, then tracks around the "seed" are nucleated to find the primary vertex.
A comparison between the two methods shows that the "stand alone" vertexing is inefficient for short lifetimes, but allows the reconstruction of decays with missing neutrals (ν, π^0, etc..) and does not require specific decay modes for the skims. On the other hand the candidate driven method has the advantage to allow the identification of primary vertices with even only one track belonging to them. In addition its efficiency at short lifetime is definitively better.

2.2 Vertex cutting tools

Various cuts are used to reconstruct and select the primary and secondary vertices. I will discuss them here briefly:

- *a. The detachment cut* $\ell/\sigma_\ell > N$. ℓ is the distance in the space between the primary and the secondary vertex. This cut is very usefull in enhancing the signal with respect to the background. Its effectiveness is weakened of course if the lifetime is very short.

- *b. Pointing back to primary.* We impose a cut on d/σ_d, where d is the distance in the space between the primary vertex and the direction of the momentum vector of the reconstructed charmed state.

- *c,d. Secondary vertex confidence level* and *primary vertex confidence level.* They concern cuts on the confidence level of the vertex fits.

- *e. No charm daugther in primary vertex.* We require a very low probability that tracks, produced in the charm decay, belong to the primary vertex.

- *f. No extra tracks near the secondary vertex.* In this case we impose a lower cut on the distance between the secondary vertex and extra tracks.

These last two requirements, which are usually called "isolation cuts", are particularly important to select charmed particles with short lifetime.

2.3 The reduced proper time

The detachment cut distorts heavily the proper time $t = \ell/\beta\gamma c$. Then to extract the lifetime a strong correction function f(t) is needed. f(t) is evaluated by means of MC simulations, which in any case involve some uncertainties on the assumed parameters and corrections, and produces systematic biases. As a consequence it is suitable to reduce as much as possible the weight of the corrections.
An important improvement can be achieved by replacing the proper time with the reduced proper time

$$t' = t - t_{min} = \frac{\ell - N\sigma_\ell}{\beta\gamma c} \tag{1}$$

where N is the significance of the detachment cut, which has been adopted. If σ_ℓ is independent of ℓ [as it can be assumed in a restricted range, at least] we succeed, to restore the exponential dependence $e^{-t'/\tau}$, using t'.
f(t') is very weakly dependent on t'. Then the systematic errors connected to it are drastically reduced.
Two t' distributions are used to measure the lifetime; they concern the signal region and the background events, respectively. The signal region is typically chosen as a region $\pm 2\sigma_m$ wide around the mass mean value M of the charm signal.
The t' distribution from the background is obtained from the sidebands, chosen not too far away from the signal region, because the background time evolution can depend on the invariant mass. Typical sidebands are two regions, $2\sigma_m$ wide, $4\sigma_m$ far from the signal peak.

2.4 The Maximum Likelihood Functions

The Maximum Likelihood Functions usually used to fit the lifetime are: the binned M.L.F. and the continuous M.L.F.

2.4.1 Binned Maximum Likelihood

The Binned M.L.F. is based upon the Poisson probability of observing s_i signal events in a bin i centered around t_i', when n_i events are predicted, in presence of B_i background events.
The number of events in the bin i of the t_i' signal distribution can be written in the following way:

$$n_i = S \times P^s(t_i') + B \times P^{bg}(t_i') \tag{2}$$

S= total signal events in the signal region; B= total background events in the signal region; P^s, P^{bg}= probabilities for an event, of signal and background, respectively, to have a decay time between t_i and $t_i + \Delta t_i$.

$P^s(t_i')$ can be parametrized as $e^{-t_i'/\tau}$; $P^{bg}(t_i')$ is obtained by the sidebands.
Then:

$$n_i = S\frac{f(t_i')\cdot e^{-t_i'/\tau}}{\Sigma f(t_i')\cdot e^{-t_i'/\tau}} + B\frac{b_i}{\Sigma b_i} \tag{3}$$

b_i=number of events in the bin i of the sideband hystogram; τ and B are the fit parameters; S is constrained to be $S = N_{tot}^{obs} - B$, where N_{tot}^{obs} is the total number of events in the signal region.
Assuming a Poisson distribution of the entries in the signal distribution:

$$L_{signal} = \prod_{i=1}^{bins} \frac{n_i^{s_i}}{s_i!} e^{-n_i} \tag{4}$$

s_i= number of events in the bin i of the signal hystogram.
For the background:

$$L_{bg} = \frac{(\mu_{bg})^{\Sigma bi}}{(\Sigma bi)!} e^{-\mu_{bg}} \tag{5}$$

where

$$\mu_{bg} = B/R \tag{6}$$

and

$$R = \frac{\text{signal width}}{\text{sideband width}} \tag{7}$$

Finally the total M.L.F. is:

$$L = L_{signal} \times L_{bg} \tag{8}$$

The advantage of the Binned M.L. is that it does not need a parametrization for the background.

2.4.2 Continuous Maximum Likelihood

In this case the contribution to the likelihood is calculated for each event in the signal region.
The probability for the event i is:

$$P(m_i, t_i') = \frac{Aexp[-(m_i - M)^2/2\sigma_m]}{\sqrt{2\pi}\ \sigma_m} f(t')e^{-t_i'/\tau} + C(m_i)T_b(t_i') \tag{9}$$

- m_i, t_i' are referred to the event i;
- M is the mean value of the invariant mass;
- $T_b(t_i')$ is the t' distribution for the background events as obtained from a fit to the sidebands.

The values of A, M, σ_m, $C(m_i)$ are fixed from a fit to the invariant mass plot and the probability $P(m_i, t_i')$ is normalized to that:

$$\int_{M-2\sigma_m}^{M+2\sigma_m} P(m_i, t_i') dm_i dt_i' = 1 \tag{10}$$

Finally the M.L.F. is:

$$L = \prod_i P(m_i, t_i) \tag{11}$$

3 Measurement of the lifetime of $D_{(}^{\pm}, D_s, \Lambda_c$

A big improvement in the precision of the lifetime measurements has been achieved with the E687 data. In Figs. 1,2,3,4 the lifetime measurements are presented with the statistical errors and, when available, the systematic errors. The decay channels and the number of events in the yields for the more accurate measurements are also mentioned. The world mean values of the Particle Data Group '92 and Particle Data Group '94 are quoted; the difference between these two quotations is due only to the E687 ('94) results with full statistics. The accuracy of our present experimental knowledge of the lifetimes is: $\sim$ 1.4% for $D^{\pm}$,$\sim$ 1% for D^0, $\sim$ 3.6% for D_s, $\sim$5% for Λ_c.

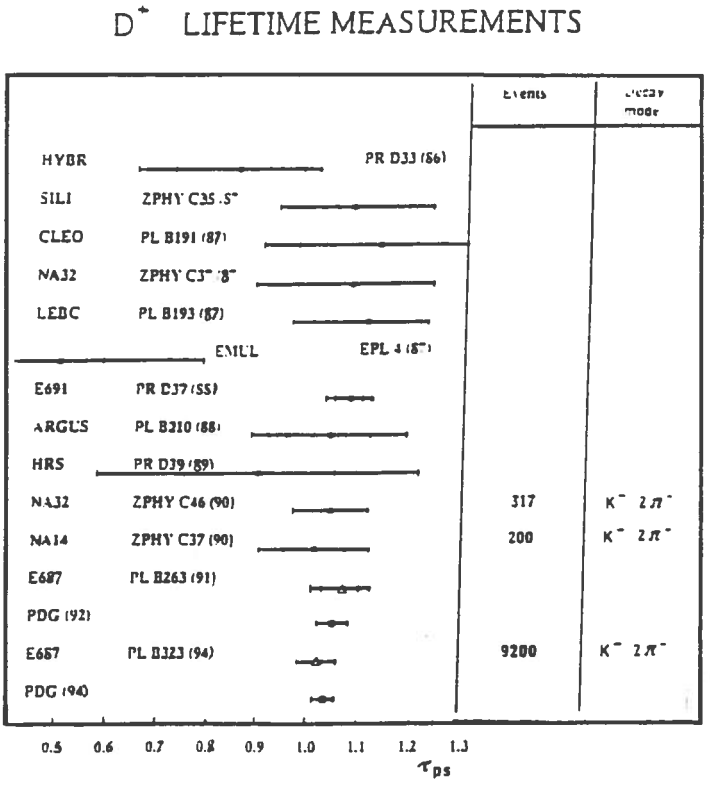

Fig. 1

D^0 LIFETIME MEASUREMENTS

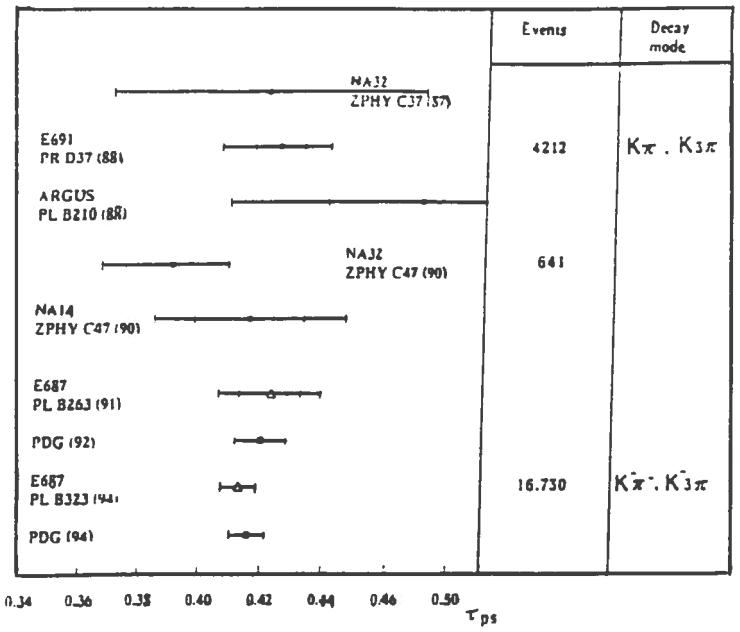

Fig. 2

D_s LIFETIME MEASUREMENTS

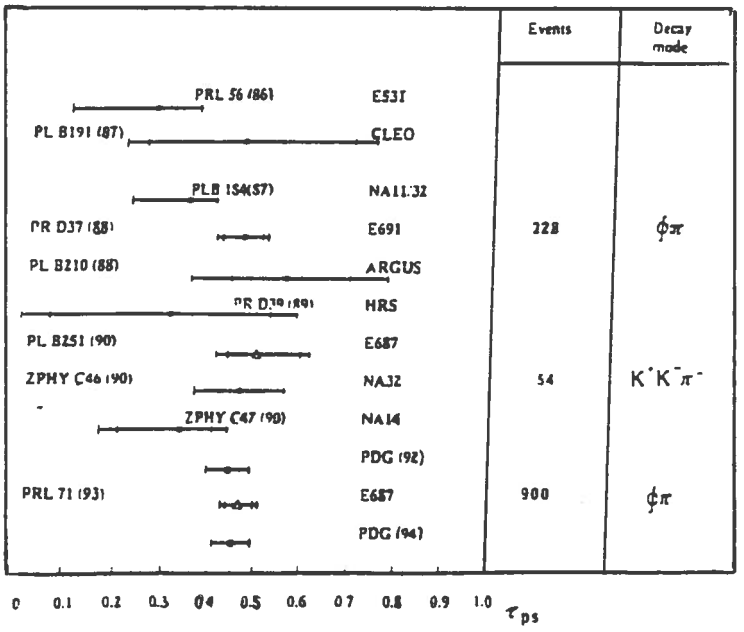

Fig. 3

Λ_c^- LIFETIME MEASUREMENTS

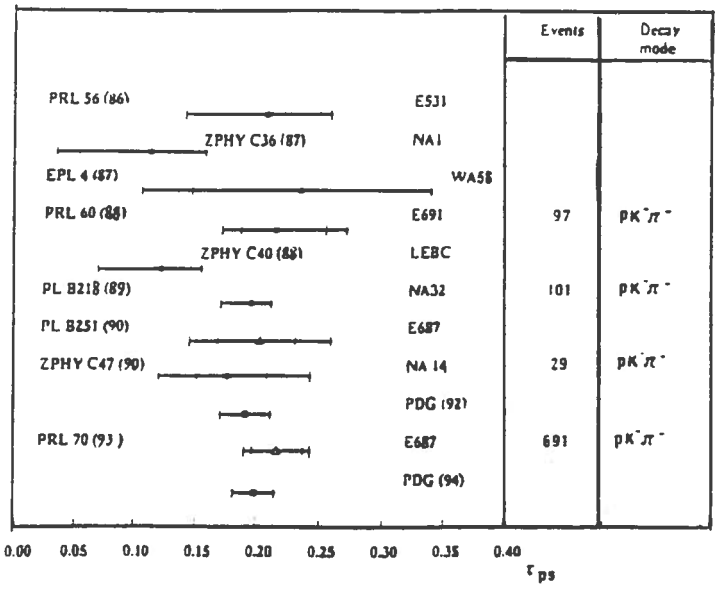

Fig. 4

In the E687 analysis a special accuracy has been devoted to the study of the systematic uncertainty. Possible contributions to the systematic errors concern the proper time distribution and the fitting procedure. The factors, which can affect the proper time distributions, are:

- the transverse profile of the photon beam;
- the momentum spectrum of the charmed states;

(both these sources are connected to possible inaccuracies of the acceptance calculations);

- the hadronic absorption of the charmed particles and their secondaries. In this case the uncertainties are due to the fact that the absorption cross section for the charmed states are unknown and, for what concern the secondaries, to the difficulty to understand to what extent the elastic scattering causes mismeasurements;
- acceptance of the detector;
- analysis cuts.

The correction function $f(t')$ is designed to account for all these factors.
Further factors affect the measured lifetime in the fitting procedure:

- the background parametrization;
- uncertainties in the calculation of $f(t')$.

In the E687 analysis the contribution of these sources to the systematic errors is very small. The best evidence of that is obtained by analyzing as $f(t')$ changes with t' and how the fitted lifetime is influenced by the choice of the detachment cut.
In Figs. 5a,b and 6a,b $f(t')$ vs t' and τ vs ℓ/σ_ℓ are presented for the D_s and Λ_c analyses.

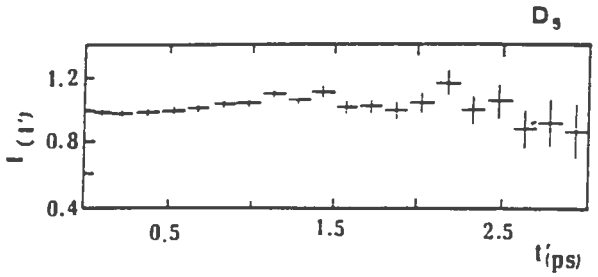

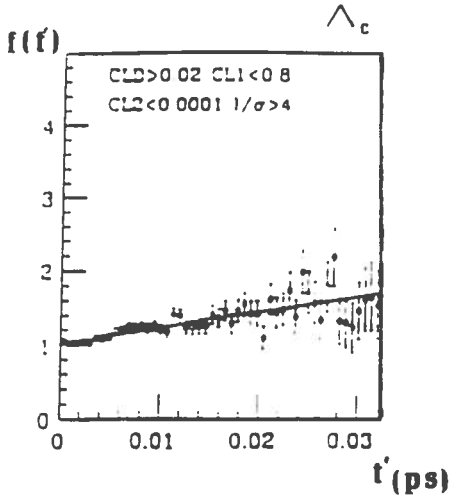

Fig. 5

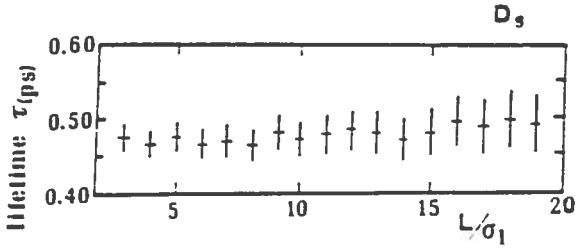

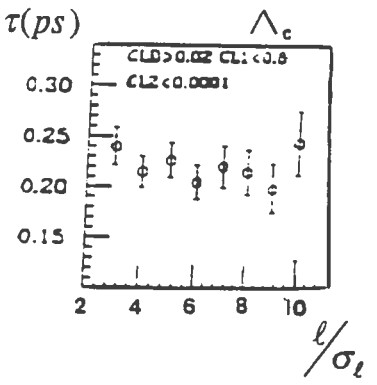

Fig. 6

We can observe that f(t') is always a very smooth function of t' and that the fitted values of the lifetime are not influenced by the detachment cut.
The systematic effects have been studied by the E687 collaboration also doing the same lifetime analyses for subsamples, defined in various ways. In Figs. 7a and 7b the results of these systematic studies are shown, as an example, for D_s and Λ_c: the lifetimes obtained by the subsamples are fully compatible with the values quoted for the full samples.

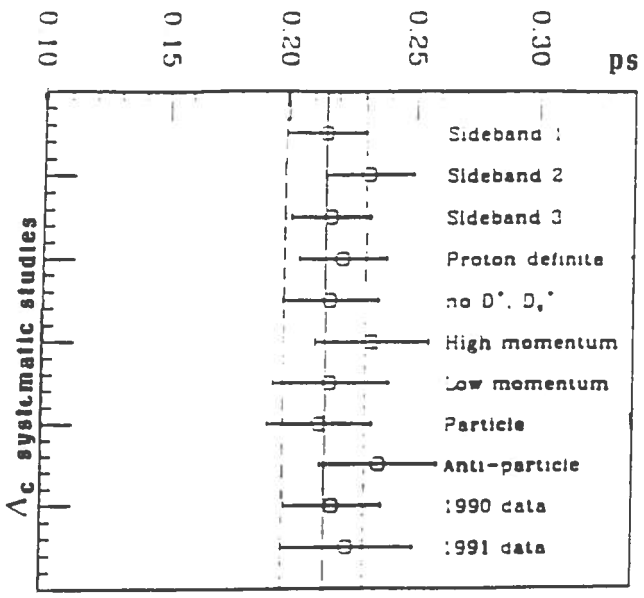

Fig. 7a

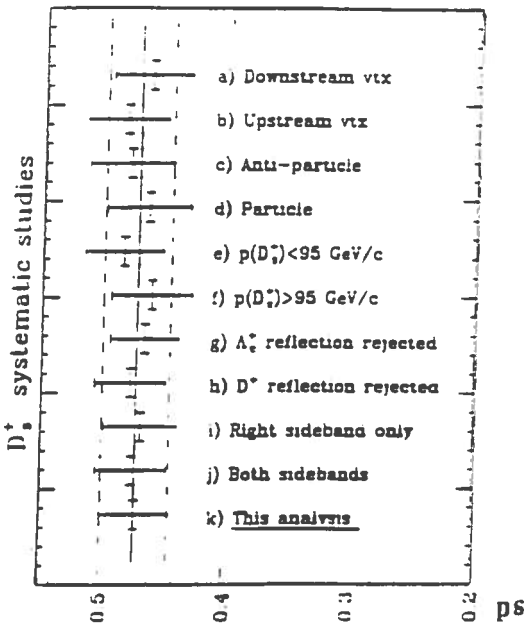

Fig. 7b

4 Study of the cascades and Ω_c^0

4.1 Ξ_c^0

In Table I a compilation of the Ξ_c^0 mass values measured up to now, are presented. The mass quoted by PDG'94 is also shown; it does not take into account the recent WA89 data.

Table I

EXPERIMENT	MODE	YIELD (events)	MASS (MeV/c^2)
CLEO	$\Xi^-\pi^+$	14	$2471 \pm 3 \pm 4$
CLEO	$\Xi^-\pi^+$	19	$2472 \pm 3 \pm 4$
NA32	$pK^-\bar{K}^{*0}$	4	$2473.3 \pm 1.9 \pm 1.2$
ARGUS	$\Xi^-\pi^+$ $\Xi^-\pi^+\pi^+\pi^-$	54	$2472.1 \pm 2.7 \pm 1.6$
E687	$\Xi^-\pi^+$	42 ± 10	$2462.1 \pm 3.1 \pm 1.4$
PDG'94			2470 ± 1.8
WA89	$\Xi^-\pi^+$	22/25	$2455 \pm 4 \pm 7$
WA89	$\Lambda K^-\pi^+$	32/37	$2465 \pm 3 \pm 7$

The Ξ_c^0 lifetime has been measured recently by E687. This is the first determination with good statistics (a previous measurement from NA32 was based on 4 events). In Fig. 8 the mass distribution for the channel studied by E687 is presented. The

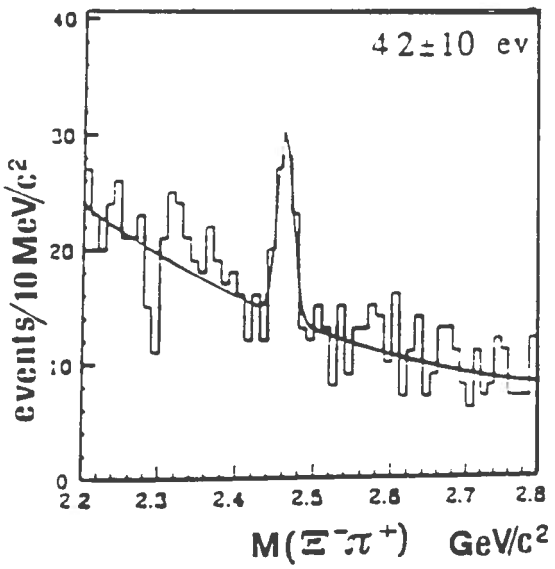

Fig. 8

decay is $\Xi_c^0 \to \Xi^-\pi^+$, where $\Xi^- \to \Lambda_0\pi^-$ and $\Lambda_0 \to p\pi^-$. In this analysis only Ξ^- decays downstream of the vertex detector are taken into account to have a high resolution track for the charmed state[1]. The yield consists of 42±10 events.
The distribution of the times of life, the correction function f(t') and τ vs ℓ/σ_ℓ are shown in Fig. 9. The correction function is very smooth and the fitted lifetime value is very stable as ℓ/σ_ℓ cut changes. This is a good demonstration that the systematic effects are small.
The Ξ_c^0 lifetime quoted by E687 is: $1.01^{+0.025}_{-0.017} \pm 0.05ps$.

5 $\Xi_c^\pm$

The charged cascade has been measured more extensively than the neutral cascade, due to its longer lifetime.
In Table II the mass measurements are presented. The PDG'94 quotation does not take into account yet the Excharm and the WA89 data. In Table III the lifetime measurements are summarized, together with the decay channel, which has been analyzed, and the statistics of signal events used to measure the lifetime.

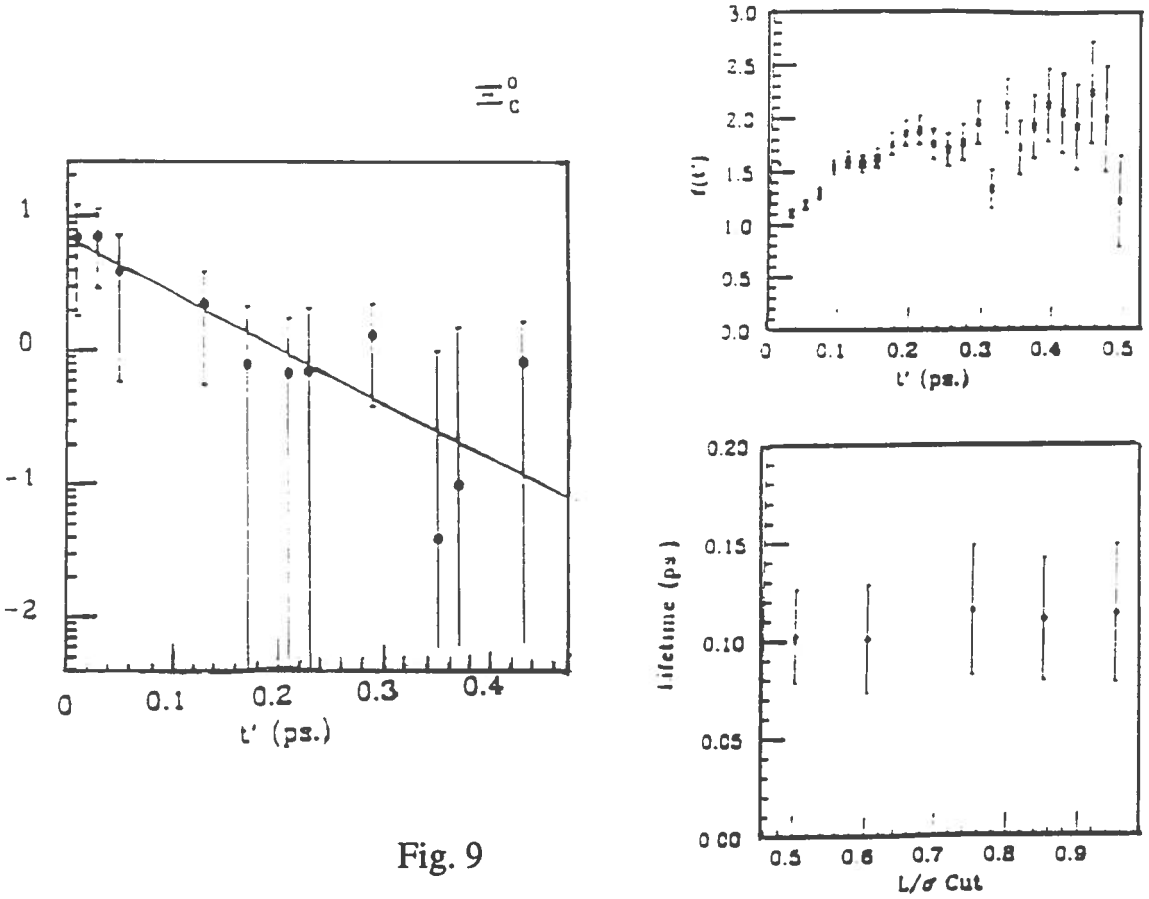

Fig. 9

Table II

EXPERIMENT	MASS (MeV/c^2)
CLEO	$2467 \pm 3 \pm 4$
ARGUS	$2465.1 \pm 3.6 \pm 1.9$
WA62	2460 ± 25
E400	$2459 \pm 5 \pm 30$
NA32	$2466.5 \pm 2.7 \pm 1.2$
E687	$2464.4 \pm 2.0 \pm 1.4$
PDG'94	2465.1 ± 1.6
Excharm	2465 ± 4
Excharm	2472 ± 4
WA89	2462 ± 3
WA89	2465 ± 3

The values quoted fluctuate in a large range, but if we take into account only the more recent values, included the preliminary ones, we can observe that the mass values range within the interval 2700-2710 MeV/c^2.

6.0.1 Ω_c^0 lifetime

The E687 collaboration studied the Ω_c^0 lifetime analyzing the channel: $\Omega_c^0 \rightarrow \Sigma^+ K^- K^- \pi^+$ in both the Σ^+ decay modes: $\Sigma \rightarrow p\pi^0$ and $\Sigma \rightarrow n\pi^+$.
In Fig. 12 the two subsamples, obtained selecting the $\Sigma \rightarrow p\pi^0$ and the $\Sigma \rightarrow n\pi^+$ decay modes, are shown together with the full sample. The Ω_c^0 mass is: $M(\Omega_c^0) = 2698.8 \pm 2.5 MeV/c^2$ (width=6.4±1.9 MeV/c^2) for the sample with $\Sigma \rightarrow p\pi^0$, and $M(\Omega_c^0) = 2700.0 \pm 2.0$ (width=5.6±1.3 MeV/c^2) for the sample considering the $n\pi^+$ decay mode. Finally the full sample gives: $M(\Omega_c^0) = 2699 \pm 1.5 \pm 2.5 MeV/c^2$. The consistency is very good. The mass widths have to be compared with the resolution alone, which is 8.0±2. MeV/c^2.

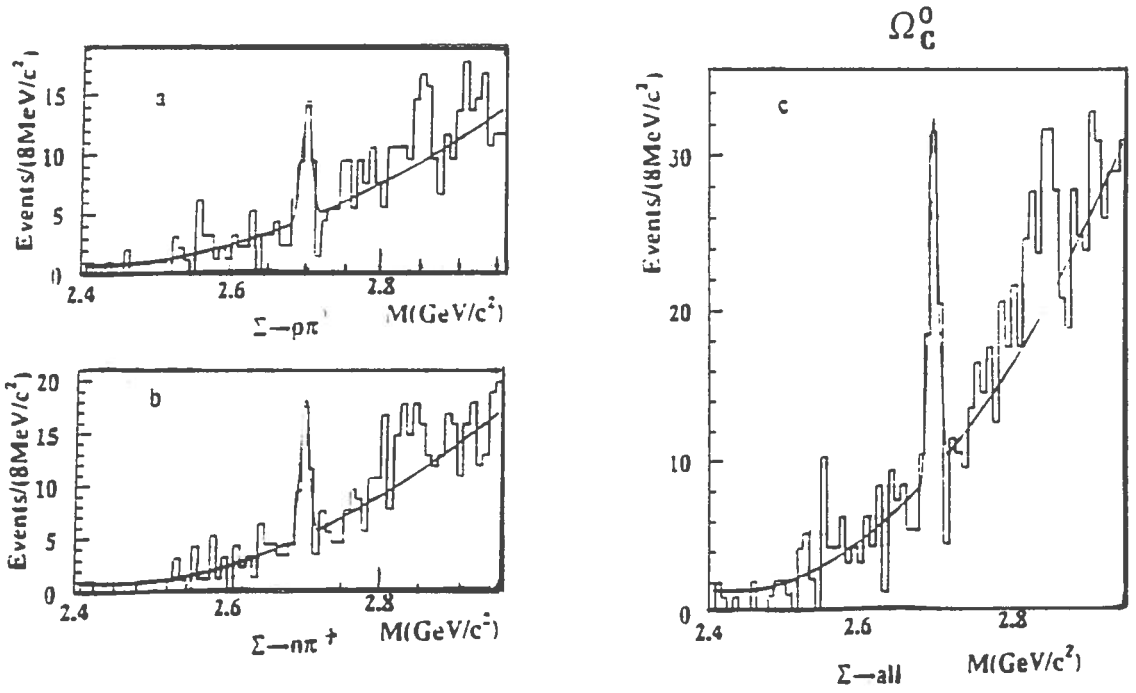

Fig. 12

In this analysis we taken into account only Σ^+ decays downstream of the vertex detector and upstream of the first magnet. In this way we can reconstruct the intersection between a high resolution Σ track (microvertex) and a p or π track (MWPC). Constraining the Σ^+ mass, $p(\Sigma^+)$ can be calculated.

6 Ω_c^0

After the first evidence provided by WA62 (with only 3 events), in 1992 ARGUS and E687 obtained a peak having ~2.7 s.d. of statistical significance in the channels $\Xi^- K^- \pi^+ \pi^+$ (12±7 events) and $\Omega^- \pi$ with $\Omega^- \to \Lambda^0 K^-$ (10±4 events), respectively. But later the decay channel $\Xi^- K^- \pi^+ \pi^+$ was studied by CLEO and E687, and the channel $\Omega^- \pi^- \pi^+ \pi^+$ by E687; in all three cases no evidence has been found.
More recently E687 reached a good statistical significance for the presence of Ω_c^0 in the channel $\Sigma^+ K^- K^- \pi^+$ with Σ^+ decaying both to $p\pi^+$ and $n\pi^+$. The total yield consists of ~ 42.5±8.8 events.
A further preliminary evidence has been obtained by E687 in the channel $\Sigma^+ K^- K_s^0$, with 21.34±8.3 events in the yield.
Up to this moment 4 independent evidences of Ω_c^0 were obtained, but no one channel was observed by two different experiments.
Very recently WA89[3] found good evidence for Ω_c^0 in the following channels: $\Omega^- \pi^+$, $\Omega^- \pi^- \pi^+ \pi^+$, $\Xi^- K^- \pi^+ \pi^+$, $\Xi^- K^0 \pi^+$, $\Xi^- K^0 \pi^- \pi^+ \pi^+$, $\Lambda K^- K^- \pi^+ \pi^+$, $\Lambda K^0 K^- \pi^+$.
Then now we have two channels showing an Ω_c^0 peak from the analysis of two different experiments: $\Omega^- \pi^+$ by E687 and WA89; $\Xi^- K^- \pi^+ \pi^+$ by ARGUS and WA89.
In Fig. 11 the Ω_c^0 invariant mass, as reconstructed in the various channels, are shown.

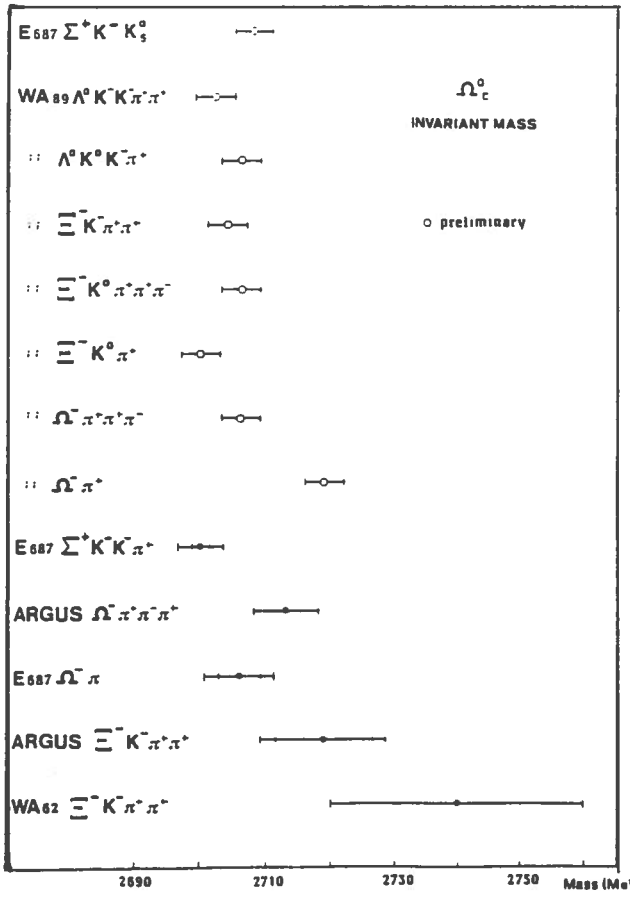

Fig. 11

Table III

EXPERIMENT	Channel	YIELD (events)	τ(ps) (MeV/c^2)
WA62	$\Lambda K^-\pi^+\pi^+$	53	$0.48^{+0.21+0.20}_{-0.15-0.10}$
E400	$\Lambda^0(\Sigma^0)K^-\pi^+\pi^+$	$5.7 \pm 15.1(\Lambda^0)$ $6.7 \pm 15.7(\Sigma^0)$	$0.4^{+0.18+0.1}_{-0.12-0.1}$
NA32	$\frac{\Xi\pi\pi}{\Sigma K\pi}$	6	$0.2^{+0.11}_{-0.06}$
PDG'92			$0.30^{+0.10}_{-0.06}$
E687	$\Xi^-\pi^+\pi^+$	29.7 ± 7	$0.41^{+0.11}_{-0.08} \pm 0.02$
PDG'94			$0.35^{+0.07}_{-0.04}$
WA89	$\Lambda^0 K^-\pi^+\pi^+$	21/18	$0.32^{+0.08}_{-0.06} \pm 0.05$

The difference between the values quoted in PDG'92 and PDG'94 is due to the E687 data.

The E687 results concern the analysis of the channel $\Xi^-\pi^+\pi^+$ with $\Xi^- \to \Lambda^0\pi^-$ and $\Lambda^0 \to p\pi^-$. Also in this case only Ξ^- decaying downstream of the vertex detector are considered.

In Fig. 10 the hystogram of the invariant masses, the plot of the times of life and of $\tau(\Xi_c^-)$ vs ℓ/σ_ℓ are shown. I would like to stress that once again the fitted lifetime values are not influenced by the detachment cut[2].

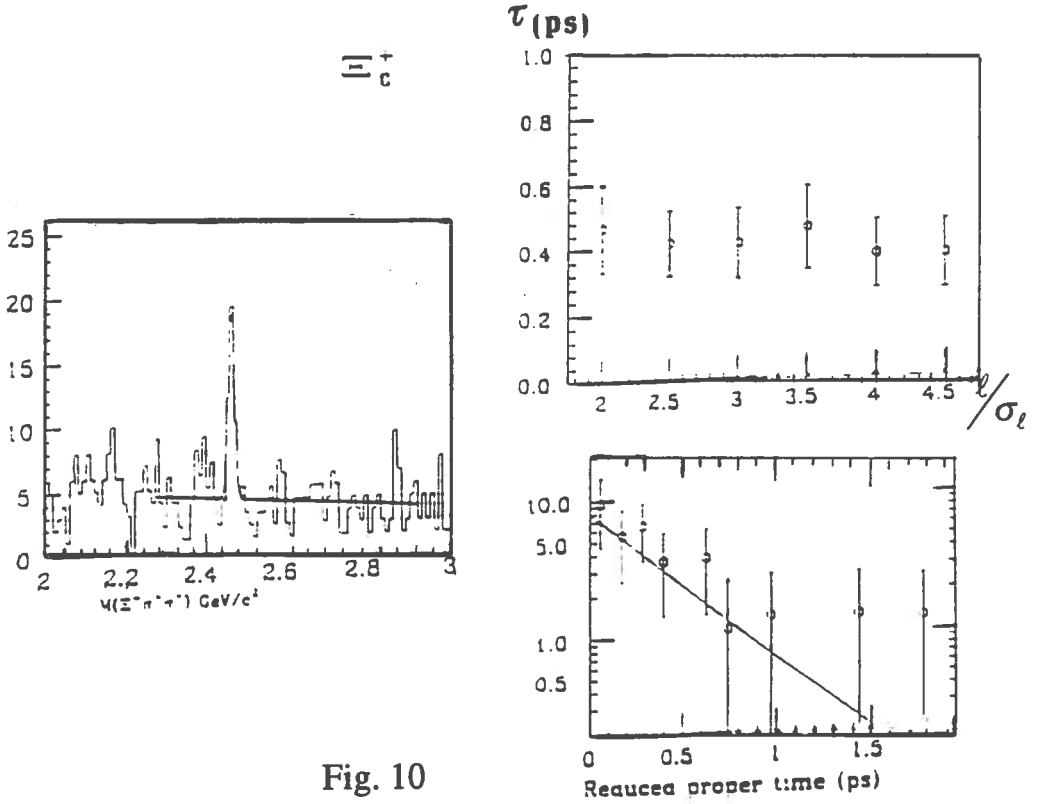

Fig. 10

The confidence level helps in solving the two-fold ambiguity, which remains at 35% for the $(p\pi^0)$ sample and at 10% for the $(n\pi^+)$ one. This difference between the two subsamples is due to the larger π^+ decay angle, if compared to the p one, and to the use of the calorimeters in checking the n direction.
Various methods are used to account for possible double candidates; the results are quite equivalent and introduce a systematic uncertainty of $\sim 0.1 MeV/c^2$. Possible contamination from other channels, as $\Xi_c^0 \to \Sigma^+ K\pi^-\pi^+$, has been studied and it has been found to be negligible.
The measurement of the Ω_c^0 lifetime presents many difficulties because, from the preliminary results, it appears to be very close to the resolution of the E687 experimental set up, which is $\sim$ 0.05 ps for the lifetime reconstruction.
As a consequence the cut on ℓ/σ_ℓ cannot be used or can be used very weakly $(\ell/\sigma_\ell > 0)$ and the simple correction function f(t') is not valid anymore. In fact the corrections obtained via MC simulations are heavily influenced by the lifetime and the resolution in t' (or t;t'≡t without detachment cuts), which have been assumed for the generation.
Various approaches are used to solve these problems. An iterative method makes use of several f(t'), calculated with different τ_{gen}. An other approach adopts a two-dimension simultaneous parametrization of $f(t', \tau_{gen})$. In addition both the Binned and the Continuous Maximum Likelihood methods are used.
The E687 collaboration has not yet given a final quotation. But what is possible to adfirm already is that the Ω_c^0 lifetime ranges between 0.05 and 0.1 ps, with a statistical error of ∼0.02 ps. The systematic error is still under study.

7 Conclusion

In Table IV I summarize the lifetime results obtained by E687, which up to now are the most accurate and in Table V their accuracy.

Table IV

	E687 λ(psec)	PDG94 λ(psec)
$D^\pm$	$1.048 \pm .015 \pm .011$	$1.057 \pm .015$
D^0	$.413 \pm .004 \pm .003$	$.415 \pm .004$
$D_S^\pm$	$.475 \pm .020 \pm .007$	$.467 \pm .017$
Λ_C^+	$.215 \pm .016 \pm .008$	$.200^{+.011}_{-.010}$
Ξ_C^+	$.410^{+.11}_{-.08} \pm .02$	$.35^{+.07}_{-.04}$
Ξ_C^0	$.101^{+.025}_{-.017} \pm .005$	$.098^{+.023}_{-.015}$
Ω_C^0	$.05 - .1$	

Table V

	Accuracy (E687)	Accuracy (PDG94)
$D^{\pm}$	1.8%	1.4%
D^{0}	1.2%	1.0%
$D_S^{\mp}$	4.5%	3.6%
Λ_C^+	8.3%	5.2%
Ξ_C^+	27.2%	15.7%
Ξ_C^0	25.2%	19.4%

The quotations of PDG'94, which include the E687 measurements, are also shown. From these results we can extract the best quotations of the ratios between D^+ and D^0, D_s and D^0 lifetimes:

$$\frac{\tau(D^{\pm})}{\tau(D^0)} = 2.547 \pm 0.043 \tag{12}$$

and

$$\frac{\tau(D_s^{\pm})}{\tau(D^0)} = 1.12 \pm 0.04 \tag{13}$$

Taking into account that the semileptonic widths, still from PDG' 94, give:

$$\frac{\Gamma(D^0 \to eX)}{\Gamma(D^+ \to eX)} = \frac{\Gamma(D^0 \to eX)/\Gamma_{tot}(D^0)}{\Gamma(D^+ \to eX)/\Gamma_{tot}(D^+)} \times \frac{\Gamma_{tot}(D^0)}{\Gamma_{tot}(D^+)} = \tag{14}$$

$$= \frac{BR(D^0 \to eX)}{BR(D^+ \to eX)} \times \frac{\tau(D^+)}{\tau(D^0)} = 1.14 \pm 0.22$$

it is clear that the extra rate of the charged D's with respect to the neutral ones is not due to the semileptonic process.

In addition the baryon lifetime hierarchy can be considered settled enough in the following way: $\tau(\Omega_c^0) \leq \tau(\Xi_c^0) < \tau(\Lambda_c^+) < \tau(\Xi_c^+)$

References

1. P.L. Frabetti et al., Phys. Rev. Lett. **70**, 2058 (1993).

2. P.L. Frabetti et al., Phys. Rev. Lett. 1381 (1993).

3. E. Chudakov - this Conference.